

Resolution of a Diastomeric Salt of Citalopram by Multistage Crystallization

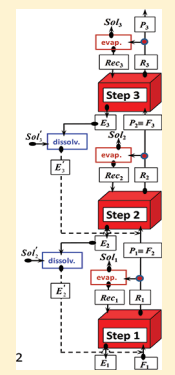
Maciej Balawejder,[†] Dawid Kiwala,[§] Heike Lorenz,[‡] Andreas Seidel-Morgenstern,[‡] Wojciech Piatkowski,[§] and Dorota Antos^{*,§}

[†]Chair of Chemistry and Food Toxicology, University of Rzeszow, Rzeszow, Poland

[‡]Max Planck Institute for Dynamics of Complex Technical Systems, Magdeburg, Germany

[§]Department of Chemical and Process Engineering, Rzeszow University of Technology, Rzeszow, Poland

ABSTRACT: Multistage crystallization has been used for resolution of the racemic mixture of citalopram to obtain pure *S*-citalopram. The racemate was converted to a diastomeric salt pair using (+)-*O,O'*-di-*p*-toluoyl-*D*-tartaric acid, (+)DTT, as a resolving agent. The obtained salts involved solid solutions almost within the entire range of the crystalline phase composition, which excluded the possibility of a single-stage resolution. Therefore, a multistep crystallization technique was employed that allowed enrichment of the racemate with the desired diastereomer in the liquid phase. Moreover, a procedure for restoring the 1:1 composition of the depleted solid phase has been developed. The procedure was based on formation of a diastomeric salt pair with the opposite enantiomer of the resolving agent, i.e., (−)DTT.



INTRODUCTION

In the past decades considerable emphasis has been placed on the use of single enantiomers versus racemic mixtures in many areas of chemistry and biochemistry.^{1–4} This was triggered by increasing awareness of the difference in the biological activity exhibited by individual enantiomers of racemic drugs.^{5,6} Two main approaches are available to produce a single enantiomer involving either resolution of racemates or stereoselective synthesis from achiral material.⁷ However, manufacturing racemates is usually more economical than stereoselective synthesis of enantiomers,⁸ particularly if efficient separation techniques can be employed allowing high yield and optical purity as well as recycling of unwanted enantiomer.^{6,9} There are a number of separation methods that can be used for optical resolution of racemates, which exploit either the enantioselective behavior of biological systems, e.g., kinetic resolutions using enzymes, or the differences in the molecular recognition of enantiomers by auxiliary chiral agents,⁶ e.g., chiral chromatography, chiral membranes, and enantioselective crystallization.⁷

In the so-called classical resolution method the enantiomers are converted to a diastomeric salt pair by reaction with a single-enantiomer resolving agent, i.e., forming a pair of diastereomers that possess the same chemical formula but have different physical properties.¹⁰ The diastereomers are then separated using crystallization, taking advantage of the differing solubility of the two components.¹¹

This method is often considered the most straightforward, economical, and easiest to perform on a large scale.^{12–14} However, discovery of an efficient resolution still often relies upon screening of a large number of resolving agents. In an

ideal situation large difference in the solubility of diastereomers is achieved.¹⁵ However, formation of double salts, for which resolution of the racemate is unfeasible, or solid solutions, where multistage crystallization is necessary to obtain substantially diastereomerically pure salts, can also be observed.^{15,16}

The solid solution type of the crystalline phase behavior has been exhibited by a system of diastereomeric salts of citalopram with the chiral resolving agent (−)-*O,O'*-di-*p*-toluoyl-*L*-tartaric acid, (−)DTT, as well as with its opposite enantiomer, (+)DTT.^{17,18}

Citalopram is an antidepressant drug belonging to the class of selective serotonin reuptake inhibitors. It is used not only to treat depression associated with mood disorders but also in the treatment of body dysmorphic disorder and anxiety.¹⁹

Citalopram is the common name for (*R,S*)-1-[3-(dimethylamino)propyl]-1-(4-fluorophenyl)-1,3-dihydroiso-benzofuran-5-carbonitrile as a racemic bicyclic phthalane derivative with chemical formula C₂₀H₂₁FN₂O.²⁰ It is supplied in the form of the hydrobromide salt. The compound has a single stereocenter, which binds a 4-fluoro(o)phenyl group and an *N,N*-dimethyl-3-aminopropyl group. Due to this chirality, the molecule exists in two enantiomeric forms. The therapeutic activity of citalopram resides in the *S*-enantiomer, commercially available with the tradename escitalopram (supplied in the form of the oxalate salt), due to its higher affinity to the human

Received: February 4, 2012

Revised: March 26, 2012

Published: April 4, 2012

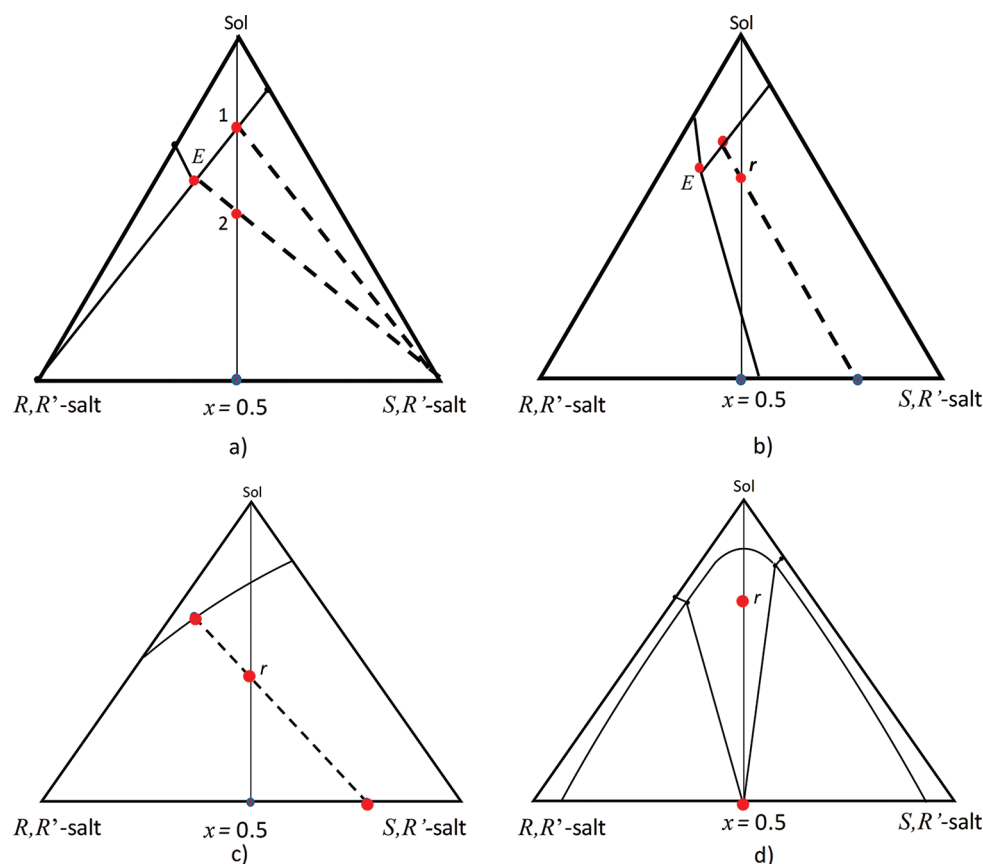


Figure 1. Illustration of the ternary phase diagrams for diastereomeric crystallization: (a) ideal solution; (1 and 2) boundary composition of the initial racemic mixture for which pure diastereomeric salt can be crystallized (e.g., S,R' salt, where R' is the R enantiomer of the resolution agent), (dashed lines) corresponding boundary conodes; (b) double salt formation; (c and d) formation of a partial or complete solid solution, respectively (1) initial racemate, (2 and 3) equilibrium compositions in the liquid and solid phase, (dashed lines) demonstration of conodes.

serotonin transporter, while the R -enantiomer is much less potent.²¹

As mentioned above, the diastereomeric salts of citalopram and $(-)$ DTT as well as $(+)$ DTT involved solid solutions in the crystalline phase. For this reason the resolution of these salts by single-stage diastereomeric crystallization was found to be unfeasible;^{17,18} it resulted in certain enrichment of 1:1 mixtures, which, however, would be required to be further increased to obtain the pure salt of the desired S -diastereomer.

In this study to separate mixtures of diastereomeric salts R,S -citalopram $\cdot(+)$ DTT multistage crystallization has been used. The principles of the procedure for multistage crystallization of solid solution forming systems have been developed in our recent study,²¹ where resolution of enantiomeric mixtures of the oxalate salt of racemic citalopram was performed. In this case, however, the separation process could not be initialized with racemic mixtures; proper enrichment of racemate with the desired S -enantiomer had to be preliminary ensured to achieve an acceptable yield and enantiomeric purity of the product.

In the case of diastereomeric salt R,S -citalopram $\cdot(+)$ DTT the initial racemic mixtures can be directly processed, where enrichment of the liquid phase with the desired diastereomer is accompanied with its depletion in the solid solution. Because a 1:1 composition of the salt mixtures is required to initialize the resolution, the solid phase with an excess of unwanted R -citalopram $\cdot(+)$ DTT (R -diastereomer) cannot be directly recycled to the process. Therefore, in this study the procedure for the multistage crystallization process was combined with

recovery of the 1:1 composition in the solid phase by diastereomeric crystallization using $(-)$ DTT.

2. CHARACTERIZATION OF THE PHASE BEHAVIOR

The design of diastereomeric crystallization has to be preceded by identification of the solid-phase behavior of the salt pair system. The most accurate method is based on determination of the ternary phase diagrams representing SLE data for mixtures of the two salts and a solvent. Demonstrations of the SLE diagrams of diastereomeric salts are presented in Figure 1.

In the case of simple eutectic resolution (Figure 1a), the pure salt of target enantiomer is obtained in the solid phase. Deviations from the simple resolution are exemplified in Figure 1b–d; they involve partial or complete solid solution in the crystalline phase (Figure 1b,c) or double salt formation, where resolution of racemate is not possible (Figure 1d). In the former case certain enrichment of the initial racemic mixture with the desired compound can be achieved in either the solid or the liquid phase depending on the nature of the solid solution, known as the Roozeboom type.²³ To achieve pure diastereomer multistage crystallization has to be used.^{22,24}

Apart from determination of the ternary phase diagram, which is time consuming, other auxiliary methods can be used for evaluation of the phase behavior such as X-ray powder diffraction (XRPD). Here, alternation of the powder patterns with a change of the solid-phase composition can be analyzed.

Another technique allowing fast determination of the solid-phase behavior of the diastereomeric system is differential

scanning calorimetry (DSC). However, applicability of the method is not general; decomposition of diastereomeric salts during heating may be a limiting factor.¹⁵

3. COUNTERCURRENT MULTISTAGE CRYSTALLIZATION FOR SYSTEMS EXHIBITING SOLID SOLUTIONS

As mentioned above, resolution of solid solution forming systems requires multistage crystallization, in which enrichment of the salt mixtures with the desired compound can be upgraded in either the solid or the liquid phase.

Details regarding the crystallization process involving a solid solution in the enantiomeric system are given in our previous study.²² The concept of a countercurrent multistage crystallization process is quoted below for the type of systems for which enrichment is upgraded in the liquid phase. The same behavior was exhibited by *R,S*-citalopram·(+)-DTT.

The idea of three-stage countercurrent crystallization is illustrated in Figure 2.

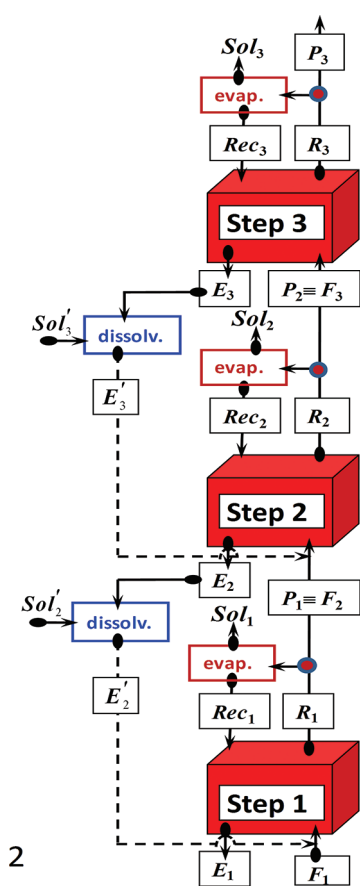


Figure 2. Flowsheet of the three-stage countercurrent crystallization process.

Each stage has two inlets, i.e., feed (F) and recycled stream (Rec), and two outlets, raffinate (R) and extract (E). The compositions of raffinate and extract streams are correlated by the SLE relationship.

The exhausted solid solution, extract, has reduced enrichment compared to the composition of the feed stream, while the enriched liquid solution, raffinate, has upgraded enrichment. A fraction of the enriched raffinate stream is recycled into the same stage after evaporation of the solvent (e.g., Sol_1 , Sol_2 ,

Sol_3 , see Figure 2), while the remaining part is delivered into the inlet of the next stage for further enrichment or is recovered as a product, P , in the last stage.

To increase the yield of operation the exhausted extract streams of each crystallization stage can be recycled into the inlets of previous stages ($n - 1$) (see Sol'_2 , Sol'_3 in Figure 2), excluding the first one, from which it is withdrawn as the fraction of waste. A graphic illustration of the countercurrent three-stage process using the ternary solubility diagram is presented in Figure 3.

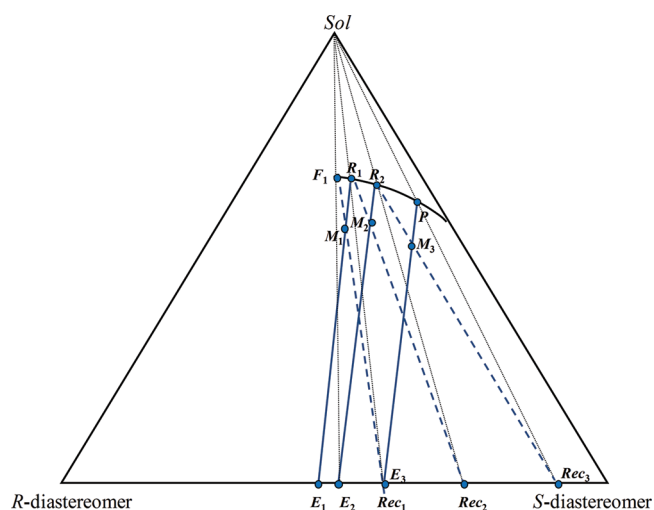


Figure 3. Graphic illustration of the three-stage crystallization process on the ternary solubility diagram: (solid lines) conodes, (dashed lines) mixing lines, (dotted lines) evaporation lines, (M) mixing points for each stage $R_n = F_{n+1} + Rec_n + Sol'_n$, $F_{n+1} = P_n$.

To realize the first run the recycled solid streams (Rec) with proper enrichment has to be delivered. However, this investment is on one-off basis; after accomplishing the first run of the multistage operation the crystallization unit can operate self-sufficiently without external delivery, excluding the feed transported to the first stage.

Such a unit can operate in the continuous as well as in the cyclic mode. In the former case the stages are directly connected, while in the latter one the units consists of several single self-sufficient stages between which the raffinate streams are transported, whereas the extract streams (E_n , $n > 1$) can be stored and used as the feed stream for the ($n - 1$)th stage at any time. Flexibility of the cyclic mode facilitates experimental realization of the process. The batch process can be realized isocratically, i.e., at the same temperature and solvent composition in each stage.

Design of the process is based on solving equations of the mass balance for each single stage (see Figures 2 and 3)

$$(F_n + E'_{n+1}) + Rec_n = M_n \quad (1)$$

$$R_n + E_n = M_n \quad (2)$$

$$(F_n + E'_{n+1}) \cdot y_{i,F_n} + Rec_n \cdot x_{i,Rec_n} = M_n \cdot y_{i,M_n} \quad (3)$$

$$R_n \cdot y_{i,R_n} + E_n \cdot x_{i,E_n} = M_n \cdot y_{i,M_n} \quad (4)$$

Note that the composition of each F_n and recycled stream E'_{n+1} is the same.

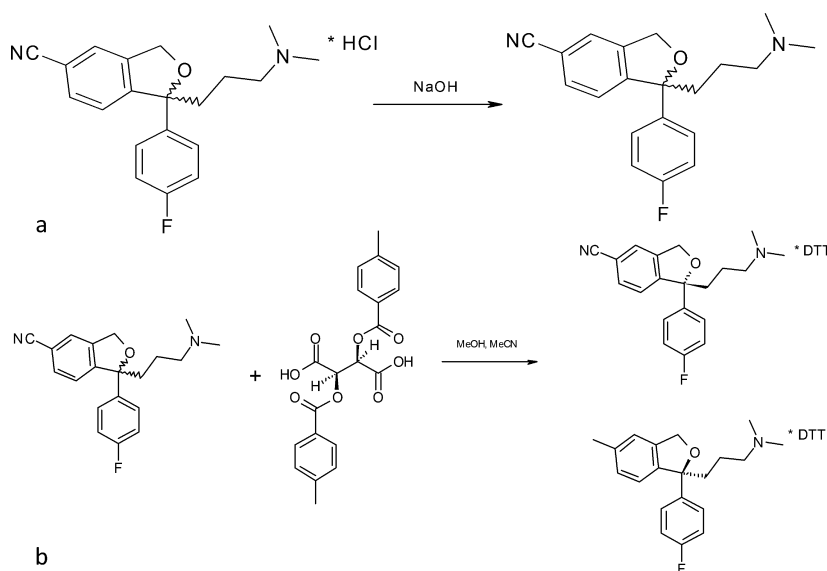


Figure 4. Synthesis route of *R,S*-citalopram(+):DTT: (a) reaction scheme of neutralization; (b) reaction scheme for formation of a diastereomeric salt pair.

The set of eqs 1–4 is coupled with the mass balance of the solid stream recycled into the same stage after evaporation expressed as

$$R_n = F_{n+1} + Rec_n + Sol_n \quad (5)$$

$$R_n \cdot y_{i,R_n} = F_{n+1} \cdot y_{i,R_n} + Rec_n \cdot x_{i,Rec_n} \quad (6)$$

and mass balance of the liquid stream recycled into the $n - 1$ stage after dissolving

$$E'_{n+1} = E_{n+1} + Sol'_{n+1} \quad (7)$$

$$E'_{n+1} \cdot y_{i,E'_n} = E_{n+1} \cdot x_{i,E_{n+1}} \quad (8)$$

where F_n is the feed (liquid) delivered to the n stage, Rec_n is the recycled stream (solid), R_n is the raffinate (liquid), E_n is the extract (solid), E'_n is the extract recycled into the previous stage after dissolving (liquid), Sol_n is the solvent, M_n is the mixing point, y_i is the mass fraction in the liquid solution, x_i is the mass fraction in the solid solution, and i denotes the component of the mixture, e.g., *R*- or *S*-diastereomer. After each stage, n , the process can be interrupted. Then, F_{n+1} denotes the product stream, P_n .

Additionally, the SLE relationship is described by functional dependencies in the following form

$$y_i = f(x_S) \quad (9)$$

If the mass of the feed stream and its composition $y_{R,F}$, $y_{S,F}$ are known, the system running in batch mode has one degree of freedom, i.e., only one process variable is available to alter the process performance.²² Note that the composition of the recycled extract streams E_n , $n > 1$ is restricted, enrichment of these streams is set the same as the feed in the previous stage. It is convenient to select the composition (i.e., enrichment) of the exhausted extract stream withdrawn from the first stage, $x_{R,E1}$, as the process variable. When the value of $x_{R,E1}$ is chosen then $y_{i,R}$ is determined by the SLE relationship and the remaining streams and their compositions, E , R , Rec , M , P , Sol , $x_{i,Rec}$, $y_{i,M}$ are calculated by solving eqs 1–8. Manipulation of the composition of the exhausted stream, $x_{S,E1}$, results in contra-

dictory changes of the performance indicators, i.e., product purity and yield. An increase of enrichment of the exhausted stream results in an upgrade of the product purity, which is counterbalanced by a reduction of the yield, and vice versa. The choice of $x_{S,E1}$ and the number of stages should be preceded by economic evaluations.

A similar procedure can be designed for solid solution systems, for which enrichment is upgraded in the solid phase. In this case, F , P , and E are the solid solutions while Rec and R are liquid.²²

4. EXPERIMENTAL SECTION

4.1. Chemicals and Equipment. The following chemicals were used in this study: racemic citalopram hydrobromide, (*R,S*)-1-[3-(dimethylamino)propyl]-1-(4-fluorophenyl)-1,3-dihydroisobenzofuran-5-carbonitrile hydrobromide with purity $Pu > 99\%$ (Jubilant Organosys Ltd.), escitalopram oxalate, (*S*)-1-[3-(dimethylamino)propyl]-1-(4-fluorophenyl)-1,3-dihydroisobenzofuran-5-carbonitrile oxalate, $Pu > 98\%$ (Yick-Vic Chemical & Pharmaceuticals Ltd.), (+)-*O,O'*-di-*p*-toluoyl-*D*-tartaric acid, (+)DTT, $Pu \geq 98\%$ (Fluka), (–)-*O,O'*-di-*p*-toluoyl-*L*-tartaric acid, (–)DTT, $Pu = 97\%$ (Sigma-Aldrich), acetonitrile for HPLC (VWR Prolabo), and methanol for HPLC (Fisher Chemical).

The laboratory equipment used in this work included the following: HPLC chromatograph (Agilent 1200 Series), thermostat (Lauda Ecoline RE-104), balance (Mettler Toledo), diffractometer PANalytical X'Pert Pro (PANalytical GmbH, Germany).

4.2. Synthesis Routes. **4.2.1. Synthesis of *R,S*-Citalopram-(+)-DTT.** The resolving agent was selected based on publications concerning resolution of racemic citalopram by diastereomeric salt crystallization,^{17,18} i.e., (+)DTT was used.

Conversion of racemic citalopram hydrobromide into *R,S*-citalopram-(+):DTT salt was realized in the following two steps: conversion of racemic citalopram hydrobromide into racemic citalopram free base, and subsequent conversion of racemic citalopram free base into *R,S*-citalopram (+):DTT salt (see scheme in Figure 4). Synthesis routes were similar to those proposed in recently published articles^{17,18} with a modification lying in the replacement of the solvent used for generation of the free base, i.e., toluene was replaced with dichloromethane.

The procedures were realized as described below.

Conversion of Racemic Citalopram Hydrobromide into Racemic Citalopram Free Base. A 20 g amount of citalopram hydrobromide

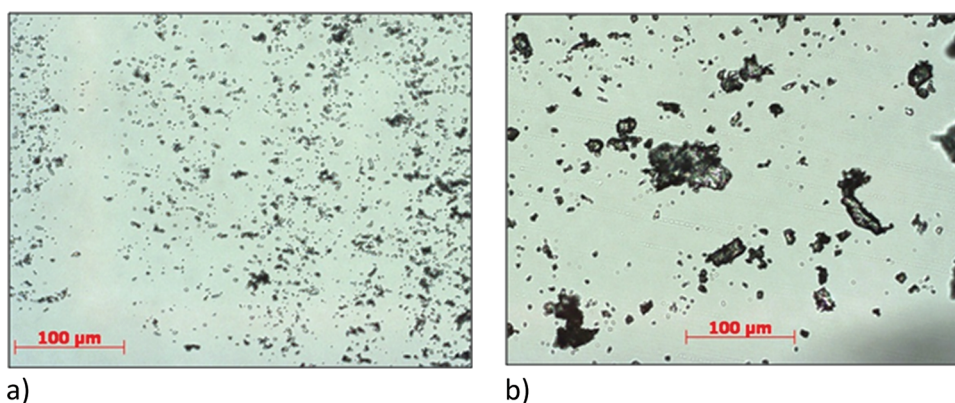


Figure 5. Microscopic photos of *R,S*-citalopram-(+)-DTT: (a) 48.3% of *S*-diastereomer and (b) 99.57% of *S*-diastereomer.

was suspended in 100 mL of water and 100 mL of dichloromethane. A 1.3 M solution of sodium hydroxide was slowly added until pH = 9.8 was achieved. This solution was intensively stirred for 45 min, and then the phases were separated. The aqueous phase was extracted using 15 mL of dichloromethane, while the organic phase was extracted using 15 mL of Milli-Q water. The organic phases were combined and dried for 2 h with anhydrous magnesium sulfate. After filtration of the drying agent, the filtrate was concentrated using an evaporator to obtain a consistency of honey. The residue of the solvent was removed by a vacuum drier ($t = 45\text{ }^{\circ}\text{C}$, $p = 0.4\text{ bar}$, time = 24 h). A reaction yield of 90% was obtained.

Conversion of Racemic Citalopram Free Base into *R,S*-Citalopram-(+)-DTT Salt in Ethanol. A 10 g amount of racemic citalopram free base was dissolved in 90 mL of ethanol by heating at $30\text{ }^{\circ}\text{C}$ in the water bath. To the mass obtained 12.4 g of (+)-DTT acid was slowly added and heated until complete dissolution was obtained. The diluted mixture was left for 6 h to crystallize at room temperature. Afterward, the solid product was separated by vacuum filtration and dried using a vacuum drier ($t = 45\text{ }^{\circ}\text{C}$, $p = 0.4\text{ bar}$, time = 48 h). A reaction yield of ca. 90% was achieved.

Due to the very low solubility of salts of *R,S*-citalopram-(+)-DTT in ethanol almost the entire amount of the salt mixture was transferred into the crystalline phase, whereas soluble postsynthesis impurities remained in the liquid phase.

This solid product was used to prepare the feed and solid solutions for the crystallization process (see section 4.6).

4.2.2. Synthesis of *S*-Citalopram-(+)-DTT. Synthesis was carried out in two steps: conversion of escitalopram oxalate into *S*-citalopram free base and next conversion of *S*-citalopram free base into *S*-citalopram-(+)-DTT.

Conversion of Escitalopram Oxalate into *S*-Citalopram Free Base. The procedure was the same as that in section 4.2.1 but instead of citalopram hydrobromide escitalopram oxalate was used. The neutralization time was shorter and lasted 30 min.

Conversion of *S*-Citalopram Free Base into *S*-Citalopram-(+)-DTT Salt in Ethanol. A 10 g amount of *S*-citalopram free base was dissolved in 30 mL of ethanol by heating at $30\text{ }^{\circ}\text{C}$ in the water bath. To the mass obtained 12.4 g of (+)-DTT acid was slowly added and heated until complete dissolution. The diluted mixture was left for 24 h to crystallize at room temperature. After this time, the solid product was separated by vacuum filtration and the residue of solvents was removed using a vacuum drier ($t = 45\text{ }^{\circ}\text{C}$, $p = 0.4\text{ bar}$, time = 48 h). The reaction yield obtained was ca. 70%.

Analogously to *R,S*-citalopram-(+)-DTT, the solubility of *S*-citalopram-(+)-DTT (*S*-diastereomer) in ethanol was low and the target product was almost entirely transferred into the crystalline phase.

This solid product was used to prepare the solid solutions for the crystallization process (see section 4.6).

4.2.3. Synthesis of *R,S*-Citalopram(-)-DTT Salt. Synthesis of *R,S*-citalopram(-)-DTT salt was performed in two steps: conversion of *R,S*-citalopram-(+)-DTT into *R,S*-citalopram free base, and subse-

quently, conversion of *R,S*-citalopram free base into *R,S*-citalopram(-)-DTT salt.

Conversion of *R,S*-Citalopram-(+)-DTT into *R,S*-Citalopram Free Base. A 10 g amount of *R,S*-citalopram-(+)-DTT containing 48.2% of *S*-diastereomer was suspended in 25 mL of Milli-Q water and 16.6 mL of dichloromethane. A detailed description of this procedure has been already given in section 4.2.1. The reaction yield was 83%.

Conversion of *R,S*-Citalopram Free Base into *R,S*-Citalopram(-)-DTT Salt. A 0.5 g amount of *R,S*-citalopram free base and 0.62 g of (-)-DTT acid were diluted in a defined volume of acetonitrile/methanol (1:0.08 v/v).

The obtained mass was heated at reflux for 40 min. Then, the solution was poured into the closed tube. The tube was inserted in a double-walled thermostatted vessel, and the solution was electromagnetically stirred for about 72 h at $25\text{ }^{\circ}\text{C}$ in order to establish the equilibrium. After that time, a two-phase system was obtained and the solid product was separated by vacuum filtration and dried using a vacuum drier ($t = 45\text{ }^{\circ}\text{C}$, $p = 0.4\text{ bar}$, time = 24 h). Both the solid and the liquid phases were analyzed using HPLC (see below section 4.3). The reaction yield was ca. 90%.

Because of the concrete value for the solubility of citalopram salts in acetonitrile–methanol mixtures certain amounts of both diastereomers could be exchanged between the phases, and after establishing the crystallization equilibrium the liquid phase was enriched with *R*-diastereomer while the 1:1 composition of the solid phase was restored.

4.3. HPLC Analysis. All chromatographic analyses were carried out using a Chirobiotic V column supplied from Astec Co. (particle size $5\text{ }\mu\text{m}$, column dimensions $250 \times 4.6\text{ mm}$). The chiral selector used in this column is macrocyclic antibiotic vancomycin. The mobile phase (eluent) composition was as follows: methanol:triethylamine:anhydrous acetic acid (99.9:0.06:0.055 v/v). Measurements have been performed at a flow rate of 1 mL/min at $25\text{ }^{\circ}\text{C}$ with an injection volume of $5\text{ }\mu\text{L}$. The UV signal was recorded at a wavelength of 240 nm.

Samples for HPLC analysis were prepared by dissolution in the eluent. The samples of the dried solid solution were prepared by dissolving up to a concentration of 1 g/L, whereas liquid solution was sampled in an amount of 0.5 mL and diluted 10–100 times. The concentration of both the liquid and the solid solutions was determined by detector calibration.

4.4. SLE Measurements of *R,S*-Citalopram-(+)-DTT. **4.4.1. SLE Experiments.** Solubility experiments were carried out for mixtures with different diastereomeric enrichment, de. Samples were prepared using the required composition of *S*- and *R,S*-citalopram-(+)-DTT (synthesized as described in section 4.2.1) and suspended in 4 mL of acetonitrile/methanol solvent (1:0.08 v/v) in closed glass vials. All samples were heated up to $60\text{ }^{\circ}\text{C}$ in a water bath until complete dissolution. Next, these vials were inserted in a double-walled thermostatted vessel, and solutions were electromagnetically stirred for about 72 h at $25\text{ }^{\circ}\text{C}$ in order to establish the liquid–solid equilibrium.

After establishing equilibrium samples of the saturated solution were centrifuged ($t = 25\text{ }^{\circ}\text{C}$, $V = 1000\text{ rpm}$, time = 2 min) and separated using a syringe with a filter. Solid phases were washed using cold ethanol, separated by vacuum filtration, and dried in a vacuum drier ($t = 45\text{ }^{\circ}\text{C}$, $p = 0.4\text{ bar}$, time = 24 h). Solid and liquid phases collected during the solubility experiments were analyzed by HPLC.

The SLE equilibrium was also identified in very close vicinity to a 1:1 composition of salt mixtures.

For that purpose, four samples with the 0.2 g of *R,S*-citalopram·(+)-DTT with composition 1:1 were prepared by dissolving in 2, 3, 4, and 5 mL of acetonitrile/methanol solvent (1:0.08 v/v) to obtain a different concentration of supersaturated solution, which corresponded to various locations of the mixing point on the 1:1 line in the ternary solubility diagram. Each of these mixing points belonged to different conodes.

Further procedure was the same as described above.

SLE measurements were repeated twice; results were found to be reproducible.

4.4.2. Additional Observations. During the investigation of SLE of *R,S*-citalopram·(+)-DTT, different crystal sizes were observed depending on the ratio of diastereomers in the samples. The solid phase with a composition of diastereomeric salts close to 1:1 was characterized by small, poorly shaped crystals (Figure 5a), whereas the solid phase with an excess of *S*-diastereomer had larger but broken crystals (Figure 5b).

Moreover, mixtures with a composition close to racemate crystallized much easier than pure *S*-diastereomer. These difficulties in crystallization of the *S*-diastereomer might be caused by the large width of the metastable zone for this diastereomer, which probably originated from its crystalline structure.

4.5. Solid-Phase Analysis by XRPD. Samples of the solid phase obtained after the SLE measurements for *R,S*-citalopram·(+)-DTT (i.e., after phase separation, washing, and drying, as described in section 4.4) were subjected to analysis by X-ray powder diffraction (XRPD) using a PANalytical X'Pert Pro diffractometer (PANalytical GmbH, Germany). The radiation source was Cu $K\alpha$. Samples were measured on Si holders and recorded in a 2-theta range of 3–40° with a step size of 0.017 and counting time of 50 s for each step.

4.6. Multistage Crystallization. The method involved preparing samples of known compositions in 50 mL closed plastic vessels. The mixture containing a defined amount of solid *S*- and *R,S*-citalopram·(+)-DTT obtained according to the procedures described above in section 4.2.1 was dissolved in acetonitrile/methanol (1:0.08 v/v). Such a feed stream was mixed with a proper mass of crystals enriched with *S*-diastereomer. Subsequently, this sample was heated up to 60 °C in a water bath until complete dissolution. Then the tube was inserted in a double-walled thermostatted vessel, and the solution was electromagnetically stirred (300 rpm) in order to establish the liquid–solid equilibrium ($t = 25\text{ }^{\circ}\text{C}$, time = 72 h). Afterward, the sample of saturated solution was centrifuged ($t = 25\text{ }^{\circ}\text{C}$, $V = 1000\text{ rpm}$, time = 2 min) and separated using a syringe with a filter. The solid phase was washed using cold ethanol, separated by vacuum filtration, and dried in a vacuum drier ($t = 45\text{ }^{\circ}\text{C}$, $p = 0.4\text{ bar}$, time = 24 h). The liquid fraction, which was enriched with *S*-diastereomer, was weighed and used as the feed stream for the next stage. The composition of both the solid and the liquid phases was determined by HPLC (see section 4.3). The same procedure was applied for the second and third stage of crystallization. The fraction of raffinate from the second stage was delivered into the third step as the feed stream, while the raffinate received after the third stage was the final product.

5. RESULTS AND DISCUSSION

5.1. Ternary Phase Diagram of *R,S*-Citalopram·(+)-DTT.

To determine the ternary phase diagram the solid–liquid equilibria for the salt pairs of *R,S*-citalopram·(+)-DTT with different composition was quantified. As mentioned above, sample mixtures were prepared by mixing proper amounts of *S*- and *R,S*-citalopram·(+)-DTT obtained by synthesis described in section 4.2. As a solvent the mixture of acetonitrile and methanol (1:0.08 v/v) was used. The composition of the

solvent was selected on the basis of solubility screening in different solvents. Use of single-component solvents such as ethanol, isopropanol, and water, resulted in very poor solubility of citalopram, whereas in methanol the solubility of *R,S*-citalopram·(+)-DTT was very high; hence, pure methanol was excluded as well. Binary mixtures methanol–acetonitrile assured proper selectivity of the separation at relatively good solubility.^{17,18}

The results of the SLE measurements in the presence of acetonitrile–methanol mixture are summarized in Table 1.

Table 1. Results of the SLE Measurements for *R,S*-Citalopram·(+)-DTT with Different d_e

before crystallization		after crystallization			
liquid phase	solid phase		liquid phase		
d_{eS} [%]	d_{eS} [%]	x_S [g/g]	d_{eS} [%]	y_R [g/g]	y_S [g/g]
0	−3.34	0.483	7.68	0.0078	0.0090
9.80	−1.40	0.493	29.2	0.0077	0.0141
19.6	−1.08	0.495	53.7	0.0053	0.0178
24.4	1.00	0.505	69.7	0.0040	0.0223
39.2	1.46	0.507	78.1	0.0032	0.0263
49.0	2.50	0.512	83.7	0.0028	0.0314
58.8	3.38	0.517	84.8	0.0031	0.0371
68.6	9.18	0.546	93.8	0.0030	0.0816
78.4	11.5	0.558	94.6	0.0025	0.0899
88.2	23.3	0.617	97.8	0.0017	0.153
93.1	43.9	0.719	99.5	0.0008	0.306
98.0	99.1	0.996	97.8	0.0070	0.627

The SLE data were marked on the ternary diagram and linked by tie lines (conodes). The obtained phase diagram is illustrated in Figure 6. As it can be seen, the data relate only to the right half of the diagram, because the measurements were started with racemate and conducted toward pure *S*-diastereomer. Conodes were concentrated within the composition range corresponding to the three-stage crystallization experiment, i.e., up to 93% of d_{eS} in the liquid phase.

The solubility diagram shows that pure *S*-diastereomer dissolves much better in the solvent compared to the racemic mixture. Furthermore, based on the shape of the ternary phase diagram, it was confirmed that *R,S*-citalopram·(+)-DTT forms the solid solution almost in the entire range of composition of the salt mixture. Moreover, the solubility curve indicates the solubility maximum for pure *S*-diastereomer, for which enrichment with the target component can be upgraded in the liquid phase. However, it was observed that the conode in the very vicinity of pure *S*-diastereomer changed the slope toward to the *S*-corner, indicating the possibility of the presence of the eutectic composition and of a narrow range for crystallization of pure *S*-diastereomer (see the phase diagram depicted in Figure 6).

The solubility measurements are also presented in a xy coordinate system (see Figure 7), which demonstrates the distribution of *S*-diastereomer between the solid and the liquid phase without solvent. As it can be observed, the *S*-diastereomer is significantly enriched in the liquid phase. This phenomenon was utilized in this study for separation of 1:1 mixtures of salts by multistage diastereomeric crystallization.

For process design the equilibrium composition of the liquid and solid phases have to be correlated. To determine proper concentration dependencies, the SLE data points presented in

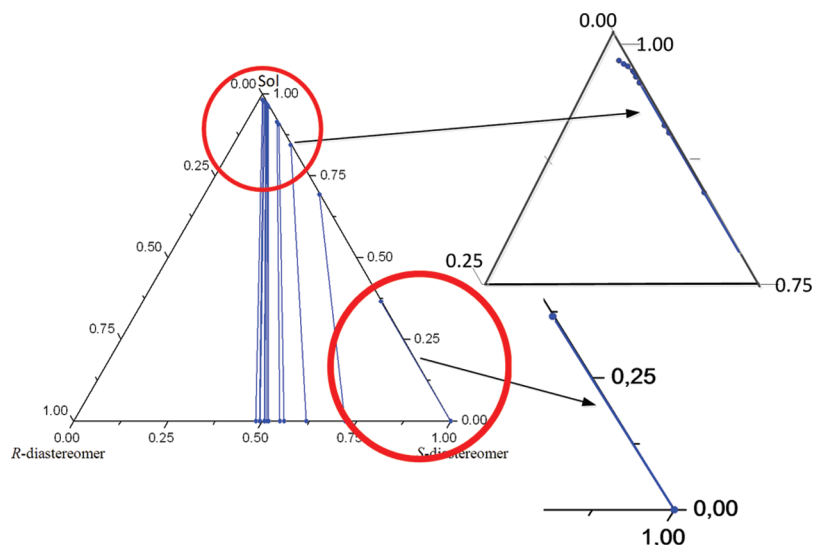


Figure 6. Ternary solubility diagram of citalopram·(+)-DTT with different de in acetonitrile/methanol at 25 °C.

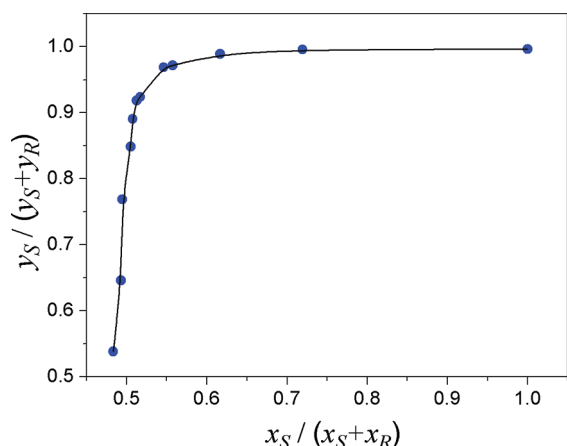


Figure 7. Distribution of S-diastereomer between the solid and the liquid phase at 25 °C.

Figure 8 were correlated by two empirical polynomial functions. To increase the accuracy of the process predictions the approximation related the data within the range selected for the crystallization experiment (i.e., upper limit was $x_S < 0.55$). The SLE relationships are given as follows

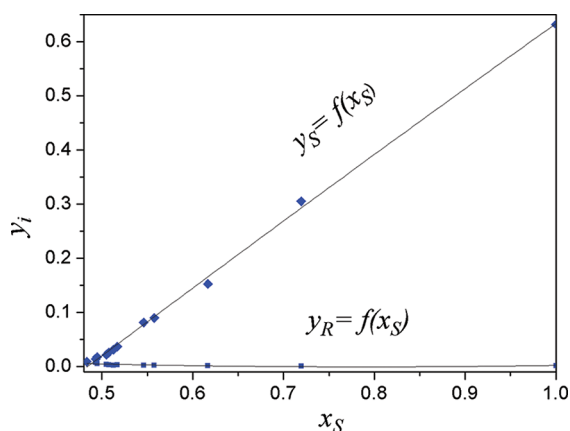


Figure 8. SLE relationship for R,S-citalopram·(+)-DTT at 25 °C.

$$y_S = -0.0583x_S^2 + 1.3139x_S - 0.6222 \quad (10)$$

$$y_R = 0.0618x_S^2 - 0.0976x_S + 0.0382 \quad (11)$$

where y_S and y_R are the mass fraction of the S- and R-diastereomer in the liquid solution, respectively, x_S is the mass fraction of the S-diastereomer in the solid solution, and the coefficient of determination $R^2 = 0.95$ and 0.92 for eqs 10 and 11, respectively.

Additionally, the SLE data in the system under study were acquired for the sample composition in the vicinity of the 1:1 composition of the diastereomeric salts. For this purpose the supersaturated solutions of 1:1 R,S-citalopram·(+)-DTT differing in concentration were subjected to crystallization. The obtained equilibrium data are presented in Table 2. It can be

Table 2. SLE Measurements in the Vicinity of 1:1 Composition of Diastereomeric Salts at 25°C

before crystallization	after crystallization				
	liquid phase	solid phase		liquid phase	
$y_S = y_R$ (1:1) [g/g]	de _S [%]	x_S [g/g]	de _S [%]	y_R [g/g]	y_S [g/g]
0.0578	-2.16	0.489	1.30	0.0082	0.0085
0.0400	-2.74	0.486	2.16	0.0088	0.0092
0.0309	-3.34	0.483	7.68	0.0078	0.0090
0.0246	-5.28	0.473	7.72	0.0080	0.0093

seen that higher enrichment of S-diastereomer in the liquid phase can be obtained by a decrease of concentration of supersaturated solutions. This indicated that the conodes in the vicinity of the 1:1 line in the ternary phase diagram differ in the slope. Those additional equilibrium data were accounted for in the SLE dependencies (see Figure 8).

5.2. XRPD Patterns of R,S-Citalopram·(+)-DTT. Due to decomposition of diastereomeric salts at the melting temperature the calorimetric measurements could not be used to identify the structure of the crystalline phase. For this purpose, XRPD solid state analysis was solely used. Samples of R,S-citalopram·(+)-DTT salts with different de were subjected to analysis. As can be observed in Figure 9, each pattern has similar reflections with the exception of the sample containing a high excess of S-diastereomer (99.57% S). Its XRPD pattern

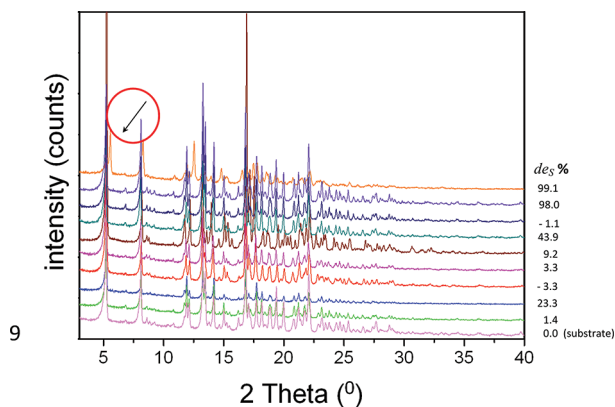


Figure 9. XRPD patterns of *R,S*-citalopram·(+)-DTT with different *de*.

reveals the existence of another crystal lattice as a new fraction. Thus, in this pattern pure *S*-diastereomer and saturated mixed crystals can be clearly identified (see additional peak shown by the arrow in Figure 9). It can be concluded that this is associated with the distinct crystallization area and the existence of a mixture close to the eutectic composition, which was identified during the SLE measurements. In the remaining cases, the absence of new phases was confirmed. Additionally, the substrates, i.e., *S*- and *R,S*-citalopram·(+)-DTT used for preparation of samples for the SLE measurements, were crystallized from ethanol and also subjected to XRPD analysis. They indicated the same structure of the crystal lattice.

On this basis, *R,S*-citalopram·(+)-DTT was defined as a solid solution forming system over almost the entire range of composition.

5.3. Multistage Crystallization. The knowledge of SLE was further exploited for designing the multistage crystallization experiment. As mentioned in section 4.6, the design was based on the fact that a *de* increase could be generated in the liquid phase. The process was realized based on the concept of the countercurrent multistage crystallization, which was explained above in section 3. It should be noted that only the first run of the three-stage process was performed with the goal of verification of the process feasibility and reproducibility of theoretical simulations. This means that the recycled streams consisted of mixtures of the solid phase with proper *de* obtained by addition of pure *S*-diastereomer to diastereomeric mixtures of salts *R,S*-citalopram·(+)-DTT with 1:1 composition. Raffinate after each stage was directly delivered into the next stage as the feed stream without partial recycling. Nevertheless, because the process is realized in a batch mode, its extension by including recycling is straightforward.

For the experiment the mass and composition of the feed stream (F_1) for the first step was set as follows: $m = 25$ g, $y_{S,F_1} = y_{R,F_1} = 0.02$. Also, the composition of the exhausted extract (x_{S,E_1}) had to be specified. Thus, for this process $x_{S,E_1} = 0.48$ was fixed. When the value of x_{S,E_1} was set the composition of both diastereomers in raffinate (y_{S,R_1}, y_{R,R_1}) was determined by the equations of the SLE relationships (eqs 10 and 11). Next, the mass of remaining streams, i.e., E_n, R_n, Rec_n, M_n , and their composition were calculated by solving the mass balance equations listed in section 3.

The diastereomeric enrichment, *de*, of the extract streams, E_n , was set the same as that of feed, F_{n-1} : $de_{E_2} = de_{F_1}$, $de_{E_3} = de_{F_2}$,

which means that no adjustment of stream composition during operation was made.

The experiment was performed according to the procedure described in section 4.6. The experimental data obtained are compared to the theoretical predictions in Table 3. Product purity and yield were used to assess the results of the performed process. The purity was measured using the HPLC system, while the yield of the desired *S*-diastereomer (Y_S) was calculated as follows

$$Y_S = \frac{m_R \cdot y_{S,R_n} - m_{Rec_n} \cdot y_{S,Rec_n}}{m_{F_n} \cdot y_{S,E_n}} \cdot 100\% \quad (12)$$

where m_{R_n} is the mass of raffinate, m_{Rec_n} is the mass of the recycled stream, and m_{F_n} is the mass of the feed stream.

On the basis of the comparison contained in Table 3 it can be concluded that the process was predictable. The observed discrepancies between theoretical and experimental masses of streams can be attributed to the very small scale of the process. Mass losses during experiment caused errors between predicted and experimental mass of the products. It could also result from small inaccuracies in the SLE measurements.

As mentioned above, product purity could be increased at the expense of a lower yield by manipulation of the composition of extract withdrawn from the first stage (x_{S,E_1}). The optimal choice of x_{S,E_1} should be done on the basis of economic evaluations.

After accomplishing all stages, the exhausted crystalline phase had reduced *de* compared to the composition of the feed stream whereas the liquid phase was enriched with the desired *S*-diastereomer. Thus, ca. 96% of *S*-diastereomer ($de_S = 90.06\%$, prediction; 92.5%, experiment) in the liquid solution was obtained after the third stage of crystallization and ca. 44% in the exhausted extract stream of the first stage. The total yield for the experiment performed was 7%. However, if the extract streams withdrawn from the all stages are recycled the yield increases markedly. For instance, single recycling of the extract stream from the second stage can upgrade the yield with a factor 1.26, double recycling 1.34, and when the extract from the first stage is also recycled 1.67. Nevertheless, in the ideal case (no mass losses), when semicontinuous processing is interrupted, 100% of the processed mixture can be recovered from all stages.

It can be observed that the first step of crystallization leads to production crystals with an excess of *R*-diastereomer, which cannot be directly recycled into the process.

Recovery of the 1:1 composition in the solid phase by simple recrystallization of depleted solutions of *R,S*-citalopram·(+)-DTT was unsuccessful; therefore, for this purpose a new procedure has been developed.

5.4. Recovery of the Racemic Composition in the Solid Phase. To increase the yield of the multistage crystallization process, recovery of the 1:1 composition of the diastereomeric salt was performed for extract E_1 that was enriched with undesired *R*-diastereomer. Recovery of the 1:1 composition from the solid solution containing 48% of *S*-diastereomer ($de_S = -3.34$) was realized in two steps. The first step was conversion of *R,S*-citalopram·(+)-DTT into *R,S*-citalopram free base, and the second one was conversion of *R,S*-citalopram free base into *R,S*-citalopram·(-)-DTT. The description of the two steps was explained in section 4.2.3.

Table 3. Experimental and Theoretical Data for the Three-Stage Crystallization

(a) data for the first stage									
theoretical and experimental inlets									
feed, F_1					recycled stream, Rec_1				
V_{solv} [mL]	mass ^a [g]	y_{R,F_1} [g/g]	y_{S,F_1} [g/g]	de_S [%]	mass [g]	x_{R,Rec_1} [g/g]	x_{S,Rec_1} [g/g]	de_S [%]	
30.7	25	0.0200	0.0200	0	0.105	0.462	0.538	7.66	
theoretical outlets									
raffinate, R_1					extract, E_1				
V_{solv} [mL]	mass [g]	y_{R,R_1} [g/g]	y_{S,R_1} [g/g]	de_S [%]	mass [g]	x_{R,E_1} [g/g]	x_{S,E_1} [g/g]	de_S [%]	Y_S [%]
30.7	24.4	0.0078	0.0091	7.66	0.693	0.5174	0.483	-3.40	33.1
experimental outlets									
raffinate, R_1					extract, E_1				
V_{solv} [mL]	mass [g]	y_{R,R_1} [g/g]	y_{S,R_1} [g/g]	de_S [%]	mass [g]	x_{R,E_1} [g/g]	x_{S,E_1} [g/g]	de_S [%]	Y_S [%]
28.9	23.1	0.0099	0.0119	9.40	0.542	0.557	0.443	-11.4	43.6
(b) data for the second stage									
theoretical inlets									
feed, F_2 (R_1)					recycled stream, Rec_2				
V_{solv} [mL]	mass [g]	y_{R,F_2} [g/g]	y_{S,F_2} [g/g]	de_S [%]	mass [g]	x_{R,Rec_2} [g/g]	x_{S,Rec_2} [g/g]	de_S [%]	
29.1	23.1	0.0078	0.0091	7.66	0.537	0.176	0.824	64.8	
experimental inlets									
feed, F_2 (R_1)					recycled stream, Rec_2				
V_{solv} [mL]	mass [g]	y_{R,F_2} [g/g]	y_{S,F_2} [g/g]	de_S [%]	mass [g]	x_{R,Rec_2} [g/g]	x_{S,Rec_2} [g/g]	de_S [%]	
28.9	23.1	0.0099	0.0119	9.40	0.537	0.176	0.824	64.8	
theoretical outlets									
raffinate, R_2					extract, E_2				
V_{solv} [mL]	mass [g]	y_{R,R_2} [g/g]	y_{S,R_2} [g/g]	de_S [%]	mass [g]	x_{R,E_2} [g/g]	x_{S,E_2} [g/g]	de_S [%]	Y_S [%]
29.1	23.283	0.0044	0.0207	64.80	0.344	0.500	0.500	0	14.3
experimental outlets									
raffinate, R_2					extract, E_2				
V_{solv} [mL]	mass [g]	y_{R,R_2} [g/g]	y_{S,R_2} [g/g]	de_S [%]	mass [g]	x_{R,E_2} [g/g]	x_{S,E_2} [g/g]	de_S [%]	Y_S [%]
27.8	22.3	0.0050	0.0235	65.0	0.361	0.509	0.491	-1.88	29.7
(c) data for the third stage									
theoretical inlets									
feed, F_3 (R_2)					recycled stream, Rec_3				
V_{solv} [mL]	mass [g]	y_{R,F_3} [g/g]	y_{S,F_3} [g/g]	de_S [%]	mass [g]	x_{R,Rec_3} [g/g]	x_{S,Rec_3} [g/g]	de_S [%]	
27.8	22.3	0.0044	0.0207	64.8	1.29	0.0497	0.950	90.1	
experimental inlets									
feed, F_3 (R_2)					recycled stream, Rec_3				
V_{solv} [mL]	mass [g]	y_{R,F_3} [g/g]	y_{S,F_3} [g/g]	de_S [%]	mass [g]	x_{R,Rec_3} [g/g]	x_{S,Rec_3} [g/g]	de_S [%]	
27.8	22.3	0.0050	0.0235	65.0	1.29	0.0497	0.950	90.1	
theoretical outlets									
product, P (R_3)					extract, E_3				
V_{solv} [mL]	mass [g]	$y_{R,P}$ [g/g]	$y_{S,P}$ [g/g]	de_S [%]	mass [g]	x_{R,E_3} [g/g]	x_{S,E_3} [g/g]	de_S [%]	Y_S [%]
27.8	23.432	0.0036	0.0682	90.1	0.171	0.462	0.538	7.66	79.7
experimental outlets									
product, P (R_3)					extract, E_3				
V_{solv} [mL]	mass [g]	$y_{R,P}$ [g/g]	$y_{S,P}$ [g/g]	de_S [%]	mass [g]	x_{R,E_3} [g/g]	x_{S,E_3} [g/g]	de_S [%]	Y_S [%]
26.1	21.9	0.0027	0.0686	92.5	0.282	0.456	0.544	8.78	52.5

^aMolar mass $M = 710$.

The obtained equilibrium data for diastereomeric salts *R,S*-citalopram·(-)DTT are summarized in Table 4.

Table 4. Result of Conversion of *R,S*- Citalopram Free Base into *R,S*-Citalopram·(-)DTT

substrate			product			
<i>R,S</i> - citalopram free base			solid phase			
y_R [g/g]	y_S [g/g]	de_S [%]	<i>R,S</i> -citalopram (-)DTT			
			x_R [g/g]	x_S [g/g]	de_S [%]	yield [%]
0.130	0.120	-3.6	0.500	0.500	0	90.2
0.104	0.096	-3.6	0.500	0.500	0	89.3
0.086	0.080	-3.6	0.498	0.502	0.40	86.6

The key point of the operation was to use (-)DTT acid and choose the appropriate concentration of *R,S*-citalopram free base (depleted with *S*-isomer) in the solvent. It is evident that the decrease of the concentration in the initial solution leads to a higher enrichment of the solid phase. Thus, starting with a nonequimolar mixture of citalopram free base, the racemic composition may be reproduced or even a small enrichment of the *S*-diastereomer can be achieved using (-)DTT.

6. CONCLUSIONS

In this study multistage crystallization was used to isolate the desired *S*-diastereomer of citalopram from racemic mixture. The process design was proceeded by measurement of the solid–liquid equilibria of diastereomeric salts *R,S*-citalopram·(+)DTT in an acetonitrile/methanol solvent system. The determined ternary phase diagram indicated that *R,S*-citalopram·(+)DTT involved solid solutions in the crystalline phase almost in the entire composition range.

Because pure *S*-diastereomer had a higher solubility than racemate, diastereomeric excess was upgraded in the liquid phase. This phenomenon was utilized in the realization of the crystallization process.

On the basis of the results of the SLE measurements a three-stage crystallization experiment was designed and successfully conducted. Nevertheless, in the first crystallization stage the enrichment of the liquid phase with the desired *S*-diastereomer was accompanied by its depletion in the solid phase. Therefore, to increase the process yield a procedure for effective recovery of the 1:1 composition of diastereomeric salts in the solid phase was developed.

The results of the experiment indicated that multistage crystallization was an efficient way to receive pure *S*-diastereomer from the racemic mixture. The total yield for the experiment performed was 7%. However, recycling of extract streams can improve the yield. Nevertheless, when the operation is interrupted or accomplished, 100% of the processed mixture can be recovered from all stages.

The advantage of diastereomeric crystallization over an “achiral approach” (i.e., without addition of the resolving agent) was the possibility of resolution of 1:1 mixtures of salts. In the achiral approach only mixtures enriched with the desired enantiomer could be resolved.²²

AUTHOR INFORMATION

Corresponding Author

*E-mail: dorota.antos@prz.edu.pl.

Notes

The authors declare no competing financial interest.

ACKNOWLEDGMENTS

The financial support of Polish Ministry of Science and Higher Education within the grant no. DPN/N135/NIEMCY/2010 is greatly acknowledged.

REFERENCES

- (1) Cayen, M. N. *Chirality* **1991**, *3*, 94–98.
- (2) Somagoni, J.; Reddy, S.; Koorelli, S.; Manda, S.; Yamsani, M. R. *Pharm. Anal. Acta* **2011**, *2*, 2–4.
- (3) Sheldon, R. A. *Chirotechnology: Industrial Synthesis of Optically Active Compounds*; Marcel Dekker Inc.: New York, 1993.
- (4) Collins, A. N.; Sheldrake, G. N.; Crosby, J. *Chirality in Industry II: Developments in the Manufacture and Applications of Optically Active Compounds*; John Wiley & Sons: Chichester, 1997.
- (5) Maier, N.; Franco, P.; Lindner, W. J. *Chromatogr., A* **2001**, *906*, 3–33.
- (6) Karamertzanis, P. G.; Anandamanoharan, P. R.; Fernandes, P.; Cains, P. W.; Vickers, M.; Tocher, D. A.; Florence, A. J.; Price, S. L. J. *Phys. Chem. B* **2007**, *111*, 5326–5336.
- (7) Li, Z.; Grant, D. J. *Pharm. Sci.* **1997**, *86* (10), 1439–1447.
- (8) Gu, C.-H.; Grant, D. J. W. Physical Properties and Crystal Structures of Chiral Drugs. In *Handbook of Experimental Pharmacology: Stereochemical Aspects of Drug Action and Disposition*; Springer: Berlin, 2003.
- (9) Rekoske, J. E. *AIChE J.* **2001**, *47* (1), 2–5.
- (10) Lorenz, H.; Sheehan, P.; Seidel-Morgenstern, A. J. *Chromatogr. A* **2001**, *908*, 201–214.
- (11) Leusen, F.; Noordik, J.; Karfunkel, H. *Racemate resolution via crystallization of diastereomeric salts: Thermodynamic Considerations and Molecular Mechanic Calculations*; Pergamon Press: New York, 1993; Vol. 49 (24), pp 5377–5396.
- (12) Collet, A. *Enantiomer* **1999**, *4*, 157–172.
- (13) Müller, S.; Afraz, M. C.; Gelder, R.; Ariaans, G. J. A.; Kaptein, B.; Broxterman, Q. B.; Bruggink, A. *Eur. J. Org. Chem.* **2005**, *6*, 1082–1096.
- (14) Ferreira, F. C.; Ghazali, N. F.; Cocchini, U.; Livingston, A. G. *Tetrahedron* **2006**, *17*, 1337–1348.
- (15) Kaptein, B.; Vries, T. R.; Nieuwenhuijzen, J. W.; Kellogg, R. M.; Grimbergen, R. F. P.; Broxterman, Q. B. New Developments in Crystallization-Induced Resolution. In *Handbook of Chiral Chemicals*; Ager, D., Ed.; CRC Press: Boca Raton, FL, 2005.
- (16) Sistla, V. S.; von Langermann, J.; Lorenz, H.; Seidel-Morgenstern, A. *Cryst. Growth Des.* **2011**, *11*, 3761–3768.
- (17) Dancer, R. J.; de Diego, H. L. *Org. Process Res. Dev.* **2009**, *13* (1), 23–33.
- (18) Dancer, R. J.; de Diego, H. L. *Org. Process Res. Dev.* **2009**, *13* (1), 38–43.
- (19) Parker, N.; Brown, C. *Ann.Pharmacother.* **2000**, *34* (6), 761–771.
- (20) Aronson, J. *Meyler's Side Effects of Psychiatric Drug*; Elsevier: Amsterdam, 2009.
- (21) Schatzberg, A.; Nemeroff, C. *The American psychiatric publishing textbook of psychopharmacology*; American Psychiatric Publishing, Inc.: Washington, D.C., 2009.
- (22) Balawejder, M.; Galan, K.; Elsner, M.; Seidel-Morgenstern, A.; Piatkowski, W.; Antos, D. *Chem. Eng. Sci.* **2011**, *66*, 5638–5647.
- (23) Sloan, G. J.; McGhie, A. R. *Techniques of melt crystallization*; J. Wiley & Sons: New York, 1988.
- (24) Lin, S. W.; Ng, K. M.; Wibowo, C. *Comput. Chem. Eng.* **2008**, *32*, 956–970.